

Three patients with defects in interferon gamma receptor signaling: A challenging diagnosis

To the Editor,

Mendelian susceptibility to mycobacterial disease (MSMD) is a rare inherited disorder characterized by infections with weakly virulent mycobacteria in otherwise healthy individuals.¹ MSMD is caused by genetic defects in genes coding for proteins in the IL-12/IFN- γ signaling pathway.²⁻⁴ IFN- γ R1 deficiency is a common cause of MSMD.^{1,5-7} The pathogenic variants in *IFNGR1* can be either autosomal recessive (OMIM #209950) or dominant (OMIM #615978),⁸ resulting in complete or partial functional defects.⁷ Lack of surface expression leads to a complete loss of function. Expression of hypomorphic or amorphic IFN- γ R1 can lead to either partial loss of function or have a dominant negative effect by impairing the wild-type allele. Complete loss of function in IFN- γ R signaling results in severe mycobacterial infections in early childhood and poor survival, while variants with partial loss of function may result in a milder clinical phenotype that manifests later in childhood. A general approach in diagnosing patients with MSMD has been proposed in the literature using flow cytometry, lymphocyte immunophenotyping, and sequencing of genes known to be involved in mycobacterial host immunity.^{7,9} However, since recent advances in genomic analysis technologies, a genotype-first approach for patients with a suspicion of an inborn error of immunity has currently become a more typical approach.¹⁰ While having the advantage of analyzing multiple genes simultaneously, some variants can be missed and the interpretation of the significance of novel variants or new combination of hypomorphic variants can be a diagnostic challenge. Here, we describe three patients with MSMD with novel or new combinations of hypomorphic variants in which functional assays were crucial to determine the extent of the interferon gamma receptor signaling defects.

Patient 1 is a 6-year-old girl who was admitted to our pediatric ward with progressive cough, fever, and tachypnea. She is the only child of non-consanguineous parents (Figure 1A). Her medical history was remarkable with more than 20 hospital admissions for bronchial hyperreactivity, lower respiratory tract infections, and a coarctectomy at the age of 2. Imaging showed mediastinal and hilar lymphadenopathy, a large right upper lobe mass and lymph nodes compressing the trachea (Figure S1). An ultrasound showed three focal lesions in the spleen and hepatomegaly. Because of her severely compromised airway, steroids were given, improving intraluminal tracheal diameter.

Histological examination on the lymph node ruled out malignant lymphoma. Sputum, stomach fluid, lymph node biopsy, and bone marrow culture revealed *Mycobacterium avium*. She was not vaccinated with Bacillus Calmette-Guérin (BCG). Plasma IFN- γ level on admission was elevated (311 pg/ml). She was treated with azithromycin, rifampicin, and ethambutol. Amikacine was added for the first 2 months. She recovered after a year of treatment. Patient 2 is a 7-year-old boy who was admitted with unexplained and recurrent low-grade fever, neck and leg pain, vasculitis-like skin lesions, and polydipsia for several months. He had a medical history with recurrent bronchial hyperreactivity, recurrent parotitis, parechovirus-associated radiculitis, and cluster headache. A brain MRI, CT scans of thorax and vertebrae, total body X-ray studies, and abdominal ultrasound showed a hypophysitis leading to panhypopituitarism, several bone lesions in skull, vertebrae and hip, hilar lymphadenopathy, and a single lesion in the spleen. Tuberculin skin test showed induration of 18mm. Cultures of a bone lesion and sputum grew *Mycobacterium persicum*. Patient 2 was also not vaccinated with BCG. Serum IFN- γ levels were undetectable. He started treatment with rifampicin, isoniazid, and ethambutol and hydrocortisone, levothyroxine, and desmopressin for his panhypopituitarism and has improved very well. Patient 3 is a 1-year-old girl with a swollen right upper arm and axillary lymphadenopathy. Her medical history showed bronchial hyperactivity and eczema. She was vaccinated for BCG during infancy and had a BCG scar that looked inflamed. A CT scan showed multiple active hilar and axillary lymph nodes, a splenic lesion and osteolytic lesions of her right humerus, two ribs, and a vertebral lesion in L2. Pathology of a bone biopsy from the right humerus showed lesions compatible with Langerhans cell histiocytosis (LCH). Treatment for multifocal LCH was started using prednisone and vinblastine. The bone lesions showed improvement, but new skin lesions appeared at the site of the BCG scar, head, and back. Repeated CT scans showed multiple bone lesions in scapulae, ribs, and progression of hilar and axillary lymphadenopathy. Skin biopsies of the lesions showed granulomatous infiltration and grew *Mycobacterium bovis* BCG strain. The previous diagnosis of LCH was re-evaluated, and a new diagnosis of BCG-osis was made. Treatment with rifampicin and isoniazid resulted in rapid improvement on skin and bone lesions and on lymphadenopathy.

A diagnostic whole exome sequencing (WES)-based PID gene panel analysis was used as first-line diagnostic approach. In Patient 1, one

This is an open access article under the terms of the Creative Commons Attribution-NonCommercial-NoDerivs License, which permits use and distribution in any medium, provided the original work is properly cited, the use is non-commercial and no modifications or adaptations are made.

© 2022 The Authors. *Pediatric Allergy and Immunology* published by European Academy of Allergy and Clinical Immunology and John Wiley & Sons Ltd.

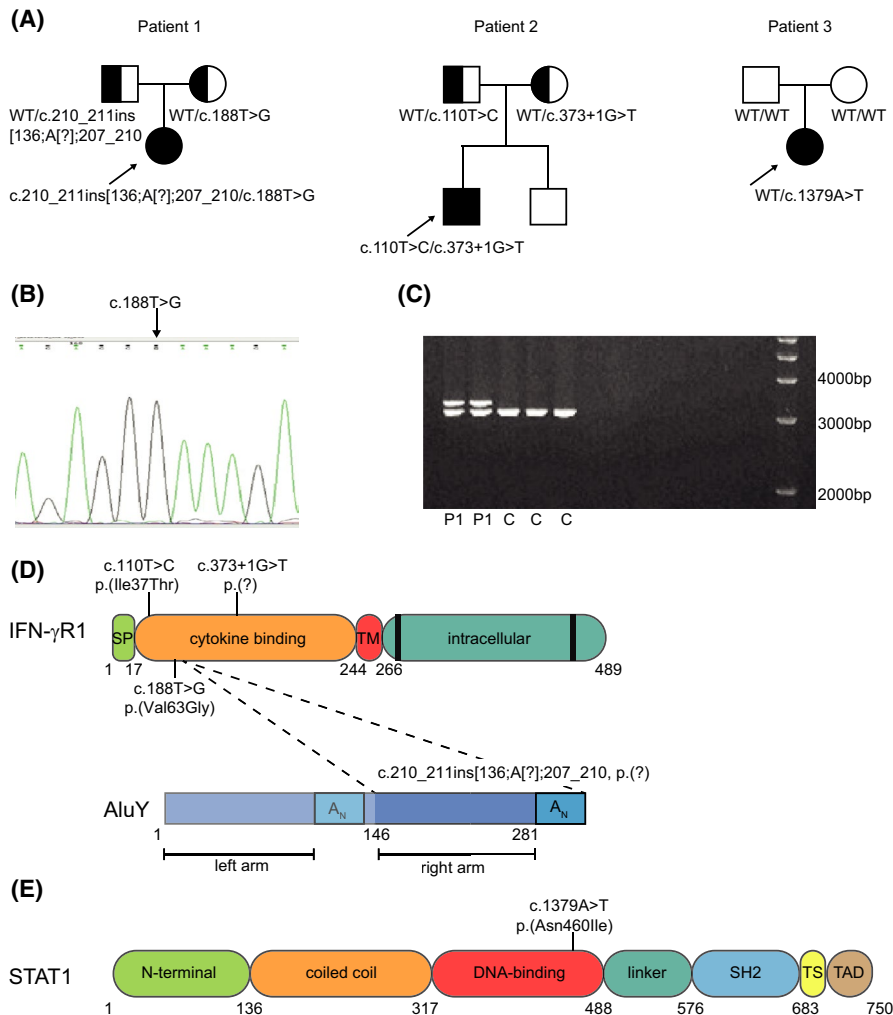


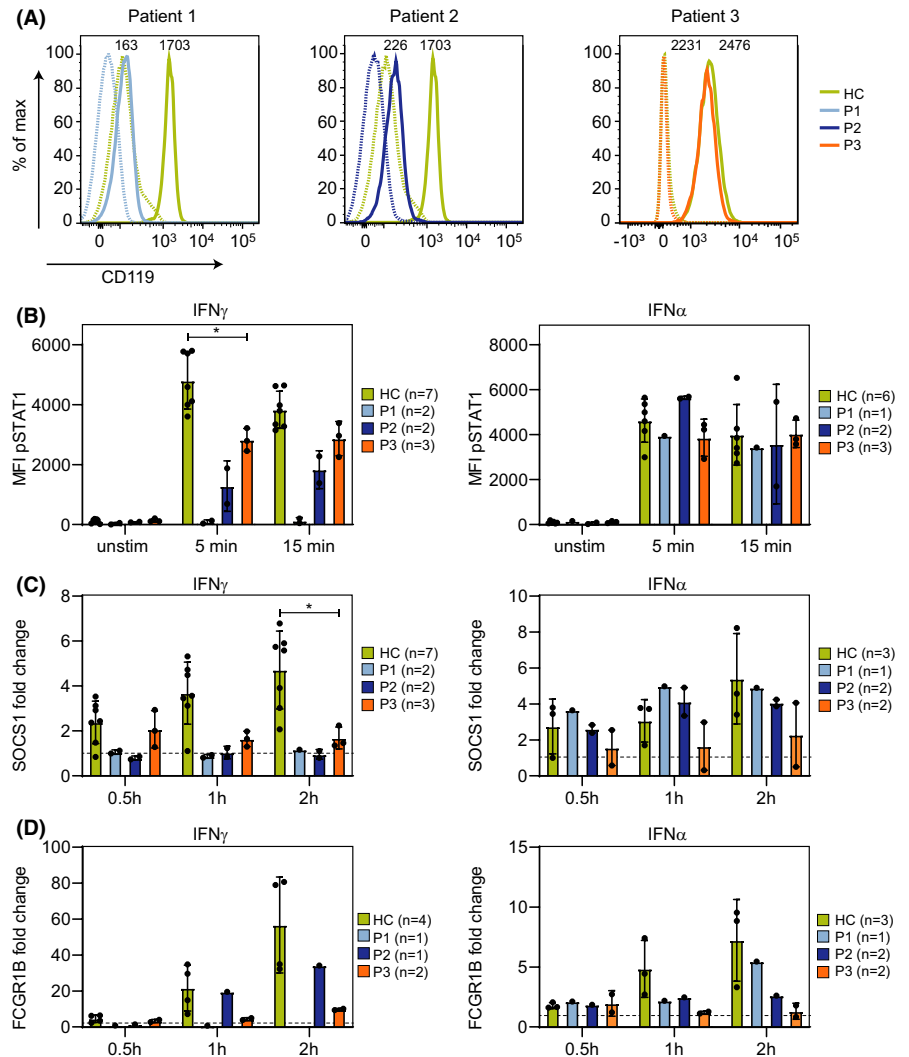
FIGURE 1 Overview of the genetic variants identified in *IFNGR1* and *STAT1*. Family pedigree of the patients indicating the genetic variant identified in the patients (A). RNA sequence analysis in Patient 1 identified only the c.188T>G variant (B). PCR using primers surrounding exon 3 on DNA derived from Patient 1 (P1) showed an additional band compared with controls (C) (C). Linear presentations of the human IFN- γ R1 (D) and STAT1 protein (E) indicating the different domains and genetic variants identified in the three patients. SP, signal peptide; TAD, transactivation domain; TM, transmembrane domain. The binding location for JAK1 and STAT1 is indicated with black lines. The numbers underneath the IFN- γ R1 and STAT1 proteins indicate the amino acid numbering. The numbers underneath the AluY transposable element indicate the nucleotide numbering of the AluY

heterozygous pathogenic variant in the *IFNGR1* gene NM_000416.2 (*IFNGR1*):c.188T>G, p.(Val63Gly) was identified. However, no second variant was detected. Interestingly, only the *IFNGR1* transcript with the p.(Val63Gly) variant was identified with RNA expression analysis (Figure 1B), and a SNP array showed decreased binding of one probe in exon 3 of *IFNGR1*. Long-range PCR using primers surrounding exon 3 showed a heterozygous insertion (Figure 1C). Sequence analysis revealed that this insertion concerned a complex insertion of 136 nucleotides of the right arm and the poly-A tail of an AluY transposable element combined with a 4-nucleotide duplication in exon 3: NM_000416.2(*IFNGR1*):c.210_211ins[136;A(?);207_210] (Figure 1D). Parental segregation analysis showed that the two variants were bi-allelic (Figure 1A). Patient 2 was compound heterozygous for a known pathogenic variant NM_000416.2 (*IFNGR1*):c.373 + 1G>T, p.(?) and variant NM_000416.2(*IFNGR1*):c.110T>C, p.(Ile37Thr), classified as probable pathogenic (Figure 1D). Parental segregation analysis showed that the two variants were bi-allelic (Figure 1A). In Patient 3, a novel variant in the *STAT1* gene: NM_007315.3 (*STAT1*):c.1379A>T, p.(Asn460Ile) was identified (Figure 1C). This variant was not identified in the gnomADv2.1.1 control populations. Parental segregation analysis showed this was a de novo variant (Figure 1A).

Functional analysis was performed to determine the effect on the IFN- γ /STAT1 signaling pathway. The surface expression of IFN- γ R1 on monocytes was severely reduced in Patient 1 and Patient 2, while the expression was normal in Patient 3 (Figure 2A). In Patient 1 and 2, the expression of STAT1 was normal (Figure S2), while the phosphorylation of STAT1 was severely reduced in response to stimulation IFN- γ , but normal upon IFN- α stimulation (Figure 2B). Furthermore, the upregulation of the IFN-gamma-regulated genes *SOCS1* and *FCGR1B* was absent after stimulation with IFN- γ (Figure 2C,D) and normal upon IFN- α stimulation (Figure 2C,D). In line with that, membrane expression of the IFN-gamma-regulated gene *CD64* was not increased after IFN- γ stimulation in Patient 2 (Figure S3). These functional data suggest that Patient 1 and 2 have a defect in IFN-gamma signaling. For Patient 1, the life-threatening presentation of disease in combination with the results of the functional analyses led to refer her for an allogeneic hematopoietic stem cell transplantation, which was successful.

The *STAT1* gene variant p.(Asn460Ile) in Patient 3 is located in the DNA-binding domain of the STAT1 protein. Studies on the crystal structure of STAT1 showed that Asn460 is important for DNA binding since it is the only amino acid that directly

FIGURE 2 Expression of IFNGR1 protein and phosphorylation of STAT1 in patient monocytes upon IFN- γ and IFN- α stimulation. Analysis of IFNGR1 (CD119, clone GIR-208) on CD14⁺ monocytes and CD3⁺ T cells showed that Patient 1 and Patient 2 had reduced expression of IFN- γ R1 in monocytes compared with the HC. The expression of IFN- γ R1 was normal in Patient 3. The MFI of CD119 in monocytes is indicated in the graphs (A) Flow cytometric analysis of phosphorylated STAT1 (pSTAT1) protein in patient monocytes after stimulation with 60 IU/ml IFN- γ or 104 IU/ml IFN- α . Each dot represents a biological replicate. (B) Expression of SOCS1 (C) and FCGR1B (D) after stimulation with IFN- γ is severely impaired in Patient 1 and Patient 2, but normal after IFN- α stimulation. In Patient 3, the expression was impaired both after IFN- γ and IFN- α stimulation. The data are represented as fold change to unstimulated. The dotted line represents 1, and each dot represents a biological replicate. The number of biological replicates are indicated for each graph



interacts via hydrogen bonds to DNA, implying that this amino acid is crucial for STAT1 function.^{11,12} In Patient 3, STAT1 protein expression was not affected (Figure S2), but the phosphorylation of STAT1 was slightly decreased (Figure 2B). Expression of SOCS1 and FCGR1B seemed normal after 0.5 h of stimulation with IFN- γ and IFN- α , but was reduced after 1 and 2 h of stimulation (Figure 2C). Together, these functional data and the fact that the variant is de novo strongly suggest that Patient 3 has an AD STAT1 deficiency.

In conclusion, patients presenting with disseminated mycobacterial infections in early or late childhood with bi-allelic or nonconclusive genetic variants in genes involved in mycobacterial immunity need to be phenotyped by functional assays of the IFN- γ /STAT1 signaling pathway in monocytes. These assays are crucial in assessing the extent of IFN- γ pathway signaling defects and in clinical decision-making.

KEYWORDS

IFN- γ receptor, mendelian susceptibility to mycobacterial disease, mycobacterial infection, SOCS1, STAT1

ACKNOWLEDGEMENT

The research for this manuscript was performed within the framework of the Erasmus Postgraduate School Molecular Medicine.

CONFLICT OF INTEREST

The authors have no conflict of interest.

AUTHOR CONTRIBUTIONS

Zijun Zhou: Data curation (equal); Formal analysis (equal); Investigation (equal); Visualization (equal); Writing – original draft (equal); Writing – review & editing (equal). **Iris H.I.M. Hollink:** Data curation (equal); Formal analysis (equal); Methodology (equal); Writing – review & editing (equal). **Arjan Bouman:** Data curation (equal); Formal analysis (equal); Writing – review & editing (equal). **Mirthe S. Lourens:** Data curation (equal); Formal analysis (equal); Writing – review & editing (equal). **Rik A. Brooimans:** Data curation (equal); Formal analysis (equal); Writing – review & editing (equal). **Tjakko J. van Ham:** Data curation (equal); Formal analysis (equal); Writing – review & editing (equal). **Peter Fraaij:** Conceptualization (equal); Investigation (equal); Writing – review &

editing (equal). **Annemarie van Rossum:** Conceptualization (equal); Investigation (equal); Writing – review & editing (equal). **Eline A.M. Zijtregtop:** Data curation (equal); Investigation (equal); Writing – review & editing (equal). **Willem A. Dik:** Conceptualization (equal); Investigation (equal); Methodology (equal); Writing – review & editing (equal). **Virgil van Dalm:** Conceptualization (equal); Investigation (equal); Writing – review & editing (equal). **Martin van Hagen:** Conceptualization (equal); Investigation (equal); Writing – review & editing (equal).

PEER REVIEW

The peer review history for this article is available at <https://publons.com/publon/10.1111/pai.13768>.

Zijun Zhou^{1,2,3}
 Iris H. I. M. Hollink^{3,4}
 Arjan Bouman^{3,4}
 Mirthe S. Lourens^{1,3}
 Rik A. Brooimans^{1,3}
 Tjakko J. van Ham⁴
 Pieter L. A. Fraaij^{5,3}
 Annemarie M. C. van Rossum^{5,3}
 Eline A. M. Zijtregtop⁶
 Willem A. Dik^{1,3}
 Virgil A. S. H. Dalm^{1,2,3}
 P. Martin van Hagen^{1,2,3}
 Hanna Ijspeert^{1,3} 
 Clementien L. Vermont^{5,3} 

¹Laboratory Medical Immunology, Department of Immunology, Erasmus MC, University Medical Center Rotterdam, Rotterdam, The Netherlands

²Division of Clinical Immunology, Department of Internal Medicine, Erasmus MC, University Medical Center Rotterdam, Rotterdam, The Netherlands

³Erasmus MC, Academic Center for Rare Immunological Diseases (RIDC), University Medical Center Rotterdam, Rotterdam, The Netherlands

⁴Department of Clinical Genetics, Erasmus MC, University Medical Center Rotterdam, Rotterdam, The Netherlands

⁵Division of Pediatric Infectious Disease and Immunology, Department of Pediatrics, Erasmus MC, University Medical Center Rotterdam-Sophia Children's Hospital, Rotterdam, The Netherlands

⁶Division of Pediatric Hemato-oncology, Department of Pediatrics, Erasmus MC, University Medical Center Rotterdam-Sophia Children's Hospital, Rotterdam, The Netherlands

Correspondence

Clementien L. Vermont, Erasmus MC, University Medical Center-Sophia Children's Hospital, PO Box 2060, 3000 CB Rotterdam, The Netherlands.

Email: c.vermont@erasmusmc.nl

Hanna Ijspeert and Clementien L. Vermont contributed equally.

Editor: Fabio Candotti

ORCID

Hanna Ijspeert  <https://orcid.org/0000-0002-7061-5321>

Clementien L. Vermont  <https://orcid.org/0000-0002-2219-856X>

REFERENCES

- Bustamante J, Boisson-Dupuis S, Abel L, Casanova JL. Mendelian susceptibility to mycobacterial disease: genetic, immunological, and clinical features of inborn errors of IFN-gamma immunity. *Semin Immunol*. 2014;26(6):454-470.
- Kerner G, Rosain J, Guerin A, et al. Inherited human IFN-gamma deficiency underlies mycobacterial disease. *J Clin Invest*. 2020;130(6):3158-3171.
- Mizoguchi Y, Okada S. Inborn errors of STAT1 immunity. *Curr Opin Immunol*. 2021;72:59-64.
- Bustamante J. Mendelian susceptibility to mycobacterial disease: recent discoveries. *Hum Genet*. 2020;139(6-7):993-1000.
- Newport MJ, Huxley CM, Huston S, et al. A mutation in the interferon-gamma-receptor gene and susceptibility to mycobacterial infection. *N Engl J Med*. 1996;335(26):1941-1949.
- Jouanguy E, Altare F, Lamhamedi S, et al. Interferon-gamma-receptor deficiency in an infant with fatal bacille Calmette-Guerin infection. *N Engl J Med*. 1996;335(26):1956-1961.
- van de Vosse E, van Dissel JT. IFN-gammaR1 defects: mutation update and description of the IFNGR1 variation database. *Hum Mutat*. 2017;38(10):1286-1296.
- Amberger J, Bocchini CA, Scott AF, Hamosh A. McKusick's Online Mendelian Inheritance in Man (OMIM®). *Nucleic Acids Res*. 2009;37(suppl_1):D793-D796. <https://omim.org/>
- Wu UI, Holland SM. Host susceptibility to non-tuberculous mycobacterial infections. *Lancet Infect Dis*. 2015;15(8):968-980.
- French MA, Tangye SG. The next generation of diagnostic tests for primary immunodeficiency disorders. *J Infect Dis*. 2019;221(8):1232-1234.
- Chen X, Vinkemeier U, Zhao Y, Jeruzalmi D, Darnell JE Jr, Kuriyan J. Crystal structure of a tyrosine phosphorylated STAT-1 dimer bound to DNA. *Cell*. 1998;93(5):827-839.
- Roy B, Zuo Z, Stormo GD. Quantitative specificity of STAT1 and several variants. *Nucleic Acids Res*. 2017;45(14):8199-8207.

SUPPORTING INFORMATION

Additional supporting information may be found in the online version of the article at the publisher's website.